RIACS

Research Institute for Advanced Computer Science
NASA Ames Research Center

On the Dynamics of Some Grid Adaption Schemes

Peter K. Sweby
Helen C. Yee

On the Dynamics of Some Grid Adaption Schemes

Peter K. Sweby
Helen C. Yee

ON THE DYNAMICS OF SOME GRID ADAPTION SCHEMES[i]

P.K.Sweby[ii] and H.C. Yee[iii]

The dynamics of a one-parameter family of mesh equidistribution schemes coupled with finite difference discretisations of linear and non-linear convection-diffusion model equations is studied numerically. It is shown that, when time marched to steady state, the grid adaption not only influences the stability and convergence rate of the overall scheme, but can also introduce spurious dynamics to the numerical solution procedure.

1. INTRODUCTION

It has been shown recently by the authors and others (see e.g. [1-4] and references therein), that the dynamics of the numerical discretisations of non-linear differential equations (DEs) can differ significantly from that of the original DEs themselves. For example, the discretisations can possess spurious numerical steady-state solutions and spurious high order period solutions (oscillatory behaviour) which may be stable or unstable (but still affecting the allowable initial data which will converge to the stable steady-state solutions) and can occur below or above the linearised stability limit on the time step for the numerical scheme. These studies are particularly important for computational fluid dynamics (CFD) since it is common practice to use a time-dependent approach to obtain steady state numerical solutions of complicated steady fluid flows. References [1-

---

[ii]Lecturer, Department of Mathematics, University of Reading, Whiteknights, Reading RG6 2AX, England.
[iii]Senior Staff Scientist, NASA Ames Research Center, Moffett Field, CA 94035, USA.

4] have demonstrated, using simple test cases, how such computations may converge to incorrect solutions, be non-convergent or suffer from residual plateauing.

Grid adaption is commonly used in CFD applications to economically resolve strong gradients and complex shock wave interactions. It is well known (see e.g. [5]) that some grid adaption techniques for time-dependent partial differential equations (PDEs) can experience instability, depending on the methods used in solving these grid adaption equations.

In this paper we apply techniques used in [1-4] to study the dynamics of grid adaption using the equidistribution principle for time-dependent approach to steady-state solutions of problems involving steep gradients. In a parallel study [6] use is made of the AUTO computer bifurcation package [7] to obtain bifurcation diagrams for similar grid adaption methods for the steady PDEs. However, the dependence on known solutions of the discretised PDEs and grid equations as starting values limits its usage. In the present work we utilise the power of the highly parallel Connection Machine CM-5 to undertake a purely numerical investigation into the dynamics possible in grid adaption schemes for the time-dependent PDEs.

Section 2 discusses the equidistribution technique and weight function used. Section 3 describes the test problems whilst Section 4 presents selected results and some concluding observations.

2. GRID ADAPTION

One common criterion used for grid adaption is the equidistribution of a positive definite weight function $w(x,t)$, often taken to be some monitor of the numerical solution $u(x,t)$ of the underlying PDE. A grid $x_0 < x_1(t) < \cdots < x_{N-1}(t) < x_N$, where x_0 and x_N are fixed, equidistributes $w(x,t)$ (at time t) if

$$\int_{x_{k-1}}^{x_k} w(x,t)dx = \int_{x_k}^{x_{k+1}} w(x,t)dx = \frac{1}{N}\int_{x_0}^{x_N} w(x,t)dx, \qquad (1)$$

for $k = 1, \ldots N$. Here we choose a one-parameter family of weight functions

$$w(x,t) = \sqrt{1 - \alpha + \alpha u_x^2(x,t)}, \qquad \alpha \in [0,1], \qquad (2)$$

where $\alpha = 1/2$ corresponds to equidistribution in the arc-length and $\alpha = 0$ yields a uniform grid.

If we now approximate $w(x,t)$ to be constant in each interval (x_{k-1}, x_k)

we have

$$\left(\sqrt{1 - \alpha + \alpha u_x^2}\right)_{k-1/2} (x_k - x_{k-1}) = \left(\sqrt{1 - \alpha + \alpha u_x^2}\right)_{k+1/2} (x_{k+1} - x_k). \tag{3}$$

Thus given a numerical solution of the PDE we can approximate the derivatives by

$$u_x|_{k-1/2} \approx \frac{u_k - u_{k-1}}{x_k - x_{k-1}}. \tag{4}$$

Equation (3) is nonlinear in $\{x_k\}$ using (4). However, (3) is linear in $\{x_k\}$ if $\{x_k\}$ in (4) uses the existing grid. In this case we can solve the tridiagonal system (3) for a new set of $\{x_k\}$ to obtain an updated grid, the modified solution values on which may be obtained either by interpolation from the old grid or a convective update to take into account the grid movement. The majority of our computations employ this linearization of $\{x_k\}$ in (4). (Note that [6] solves a slightly different form than (3).)

Various strategies are possible using the regriding technique (3). For example, the grid adaption can be applied after every time step of solving the PDE or after a prescribed number of time step based on some criteria of the computed solutions. The $\{u_k\}$ can be updated via interpolation from the old values. If time-marching to the steady-state numerical solution is sought, crude approximations to updating solution values $\{u_k\}$ immediately following a regriding step may be made. For example interpolation from the old grid can be used even after large grid movement or no adjustment of solution values $\{u_k\}$ at all. In such cases we let the $\{u_k\}$ be adjusted by the numerical scheme itself as it converges toward a steady state.

3. TEST PROBLEMS

The test problems used in this study are linear and non-linear forms of the convection-diffusion equation

$$u_t + f(u)_x = \epsilon u_{xx} \tag{5}$$

with $f(u) = u$ and $f(u) = \frac{1}{2}u^2$ respectively. We impose boundary conditions $u(0,t) = 0$ and $u(1,t) = 1$ for the linear case and $u(0,t) = 1$ and $u(1,t) = -1$ for the non-linear case which result in steady-state solutions of a boundary layer at $x = 1$ and a viscous shock at $x = 1/2$ respectively. In both cases the steepness of the feature is governed by the parameter ϵ.

We use a method of lines approach to solve the PDE with central spatial differencing for the diffusion term and either upwind or central differencing for the convective term. The resulting system of ordinary

differential equations (ODEs) for du_k/dt is then solved using a standard numerical method for ODEs. We have experimented with various explicit methods, such as forward Euler, second and fourth order Runge-Kutta, as well as the linearised implicit (backward) Euler method. As expected the stable time step required for the explicit methods was orders of magnitude lower than that for the implicit method and so we concentrated on this latter method of solution in this paper. Note also that unlike the standard explicit Runge-Kutta methods (i.e. all but forward Euler), linearised implicit Euler cannot introduce spurious steady states. However, it can stabilise genuine unstable steady states of the system; see for example [2]. Note that for this scheme and the linear problem, any non-linearity present is due solely to the grid adaption.

The regriding strategy adopted was to regrid after every time step of the PDE method, either interpolating updated solution values from the old grid or performing no adjustment at all due to grid movement. This latter approach in effect presents the PDE method with new initial data to the problem at each step.

We performed many of our calculations on a CM-5 connection machine at NASA Ames. Its parallel architecture enabled us to easily perform computations covering a range of selected parameters, usually ϵ, but also the time step Δt and the monitor parameter α. We use nodal placement and the ℓ_2 norm of the solution to illustrate our results. In all of the computation on the CM-5, we use the previous time step value for x_k in (4) to achieve a linear tridiagonal system for the updated grid in (3).

For the majority of the results, 19 free (interior) nodes were used. Numerical experiments indicate that there is no major difference in quality of the results with either an odd or an even number of nodes. We divide a chosen parameter space (e.g., ϵ) into 512 equal intervals with the rest of parameters (α, Δt, initial data) fixed. For each chosen parameter value, we iterate the discretised PDE and the grid function 4,000 steps (8,000 steps for the explicit methods) to allow the solution to settle to an asymptotic state. Then, we perform a series of time step/regriding stages, during which we investigate the dynamics by producing an overlaid plot of the norms at each step, resulting in a bifurcation type diagram.

To examine the effect of grid adaption alone compared with the time-dependent approach to the steady states with regriding above, we also solve the regriding equations (3) and (4) iteratively using the analytic solutions of the PDE (5), starting from a uniform grid. We also used a quadrature based equidistribution applied to (1), namely the trapezium

rule with a large number of subdivisions, to obtain the "exact" placements of the grid nodes for the analytical steady-state solution.

Due to a page limitation, details of the formulas, procedures and extended results on the above will be reported in an extended version of this paper. The following summarized a small portion of the results using central difference for the convection and diffusion terms and the linearized implicit Euler method.

4. RESULTS

Although results for various values of α were computed, we focus on only a few of those obtained using $\alpha = 1/2$, but will remark on results obtained with other values towards the end of this section.

4.1 The Linear Problem.

Figure 1 shows the nodal position for the steady-state solution obtained using our regriding technique (3) iteratively on the analytic form of the solution of the PDE (5). As expected the grid is concentrated around $x = 1$ for small ϵ due to the very steep gradients of the solution there. These results agree with the "exact" nodal placements obtained by the fine quadrature equidistribution mentioned in the previous section. The figure shows a settled solution, which took between 100 iterations for the smallest value ϵ and 10 iterations for the largest. It is interesting to note that a staircase effect is observed on the plots with iterations against $\log_{10} \epsilon$ (figures not shown).

Figure 2 shows the corresponding nodal positions when the time dependent PDE is solved to steady state using central spatial differences, with no adjustment to $\{u_k\}$ after regriding. Unless we state otherwise the nodal position plots show the final 5 nodal positions for each node, overlaid on the same plot. In this particular case it can be seen that for $\epsilon > 10^{-2.6}$ the grid has settled, whilst for lower values of ϵ this is not the case. Notice the jump in nodal positions as ϵ is varied through $10^{-2.4}$. This is a phenomenon observed in many of our calculations, although the particular value of ϵ at which this would happen varied. Careful examination near $\epsilon = 10^{-3.5}$ suggests some slight structure in the pattern of nodal positions. This is revealed more clearly in Figure 3, a bifurcation diagram of the ℓ_2 norm of the solution, where a structure resembling a period seven bifurcation can be seen. For larger values of ϵ the norm of the numerical solution agrees with that of the analytic steady state.
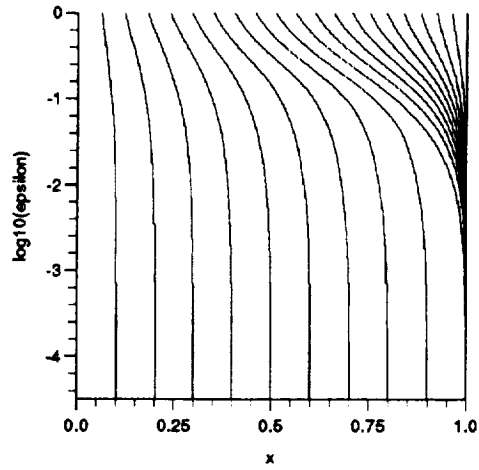
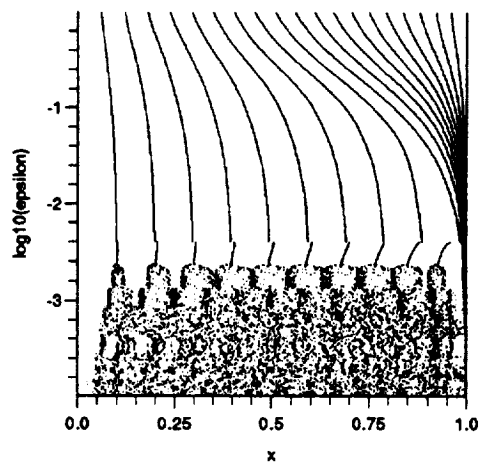Figure 1: Nodal positions for the exact linear problem using matrix iteration

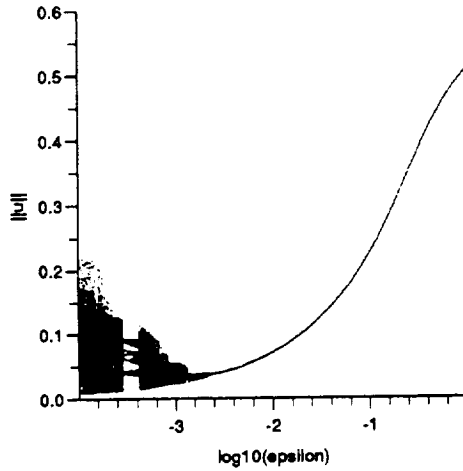Figure 2: Last 5 nodal positions for the linear problem, central differences, $\Delta t = 1$

Figure 3: Solution norm for the linear problem, central differences, $\Delta t = 1$

Figure 4 shows the bifurcation diagram for a selected range of Δt values. Note that the selected range of Δt is divided into 512 equal intervals. For each (fixed) Δt value, a fresh calculation of the discretised PDE and grid function was performed The correct solution is obtained for both large and small values of Δt, but additional spurious asymptotes occur for the range $0.1 < \Delta t < 10$. In our other work [2] we have found that this is not un-typical of the linearised implicit Euler scheme used here. The nodal positions are given in Figure 5 and agree reasonably well, where they have converged, with other results using the same value of ϵ. It is to be noted that converged nodal positions are independent of the time step Δt of the scheme.

The previous results were produced without adjusting nodal values between regriding and the subsequent time step iteration (a procedure which can only be contemplated for situations where a steady state is sought because the transient behaviour of the solution is unimportant). Figures 6 and 7 show results for the same parameter values, but where interpolation using the old grid has been used to adjust the solution values at each regriding step. As can be seen this has modified the behaviour but not completely eliminated the problem. Notice in particular how there is a greater amount of node movement compared to the norm of the solution than in the previous case. Also note that the range of Δt affected has
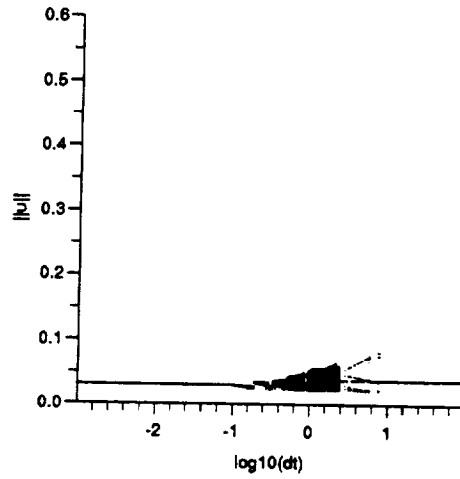
Figure 4: Solution norm for the linear problem, central differences, $\epsilon = 0.001$
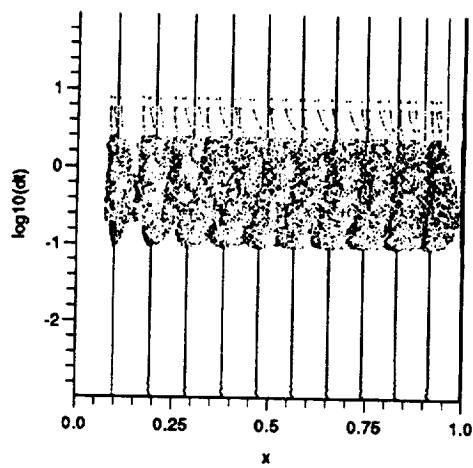

Figure 5: Last 5 nodal positions for the linear problem, central differences, $\epsilon = .001$
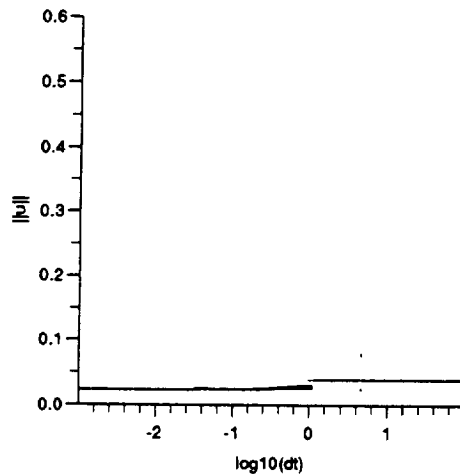
Figure 6: As Figure 4 but using interpolation

shifted.

4.2 The Non-linear Problem.

Figure 8 shows the final 5 sets of nodal positions obtained by applying the regriding technique iteratively to the analytic steady-state solution. Here the nodal positions are incorrect for small ϵ when compared with those obtained using quadrature based equidistribution. The correct positions can be visualised by extrapolating back from those for $\epsilon = 10^{-2}$. Notice again the jumps in the nodal positions as ϵ is varied. In the middle range of ϵ a period two solution can be observed for the centre three nodes. This is one case where the effect is much more pronounced for an even number of free nodes.

Much of the dynamics observed in the linear problem can be found in the non-linear case, although due to its increased severity the features are often more pronounced and convergence less readily attained. Detailed results will be reported in an extended version of this paper. To give a flavor of the dynamics for the nonlinear case, Figure 9, shows an overlaid plot of the values taken by the numerical solution itself for one set of parameter values in the range where convergence is not obtained.
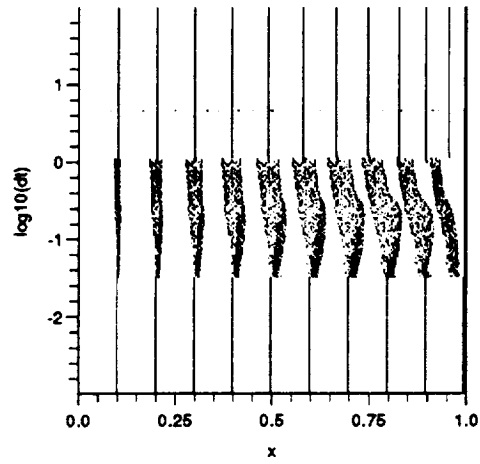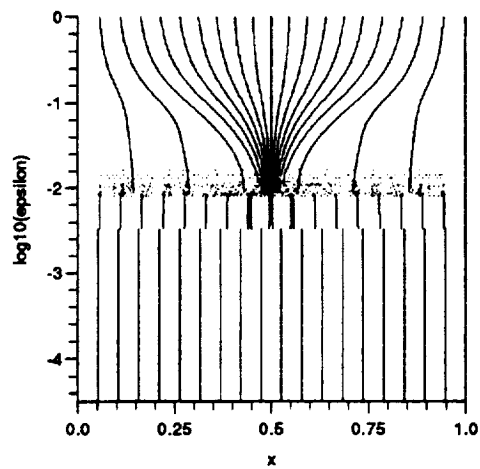
Figure 7: As Figure 4 but using interpolation

Figure 8: Last 5 nodal positions for the exact non-linear problem using matrix iteration
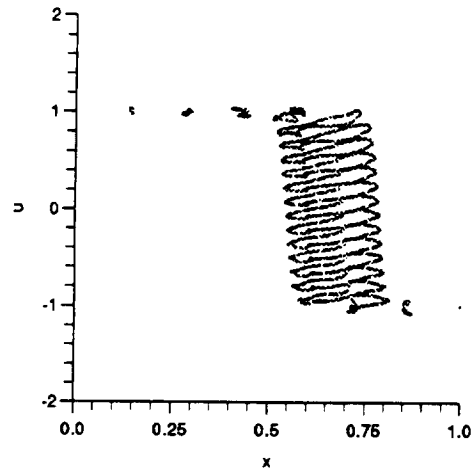
Figure 9: Superposition of last 512 solution profiles for non-linear problem, central differences, $\Delta t = 0.01$, $\epsilon = 0.01$

4.3 The effect of α.

As mentioned previously we have also carried out calculations with other values of α in our weight function (2). A value of $\alpha = 0$ yields a uniform gird, whilst $\alpha = 1$ is in general unsuitable since strict positivity of the weight function is lost. This is particularly the case in our test problems for small ϵ due to the solution gradients being very near zero. For α values other than 1, similar phenomena are encountered as for $\alpha = 1/2$. However, the nodes are more tightly clustered around the steep gradients of the solution for larger α and are more spaced out for lower α. Also, for α near 1, convergence becomes harder to obtain. There is an increase in spurious dynamics of the numerical solutions and nodal values, especially for the non-linear problem. Figure 10 illustrates some of the behaviour for the linear problem.

4.4 Concluding Remarks.

We have presented a small selection of results from our preliminary investigation into the dynamical properties of grid adaption schemes. Future research will expand on the present work, and in particular concentrate on understanding the complicated dynamical behaviour in the hope
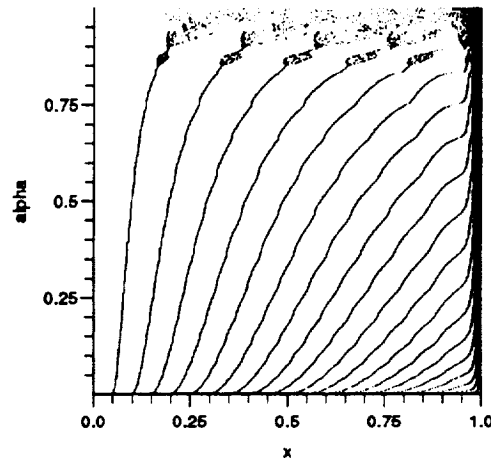
Figure 10: Dependence on α for the linear problem using interpolation, central differences, $\Delta t = 1$, $\epsilon = 0.01$

of mapping out a reliable range of grid weight functions and grid adaption parameters of commonly used numerical schemes in CFD for flows containing strong gradients.

REFERENCES

1 YEE, H.C., SWEBY, P.K., GRIFFITHS, D.F. — Dynamical Approach Study of Spurious Steady-State Numerical Solutions for Nonlinear Differential Equations, Part I, The Dynamics of Time Discretizations and its Implications for Algorithm Development in Computational Fluid Dynamics. J. Comput. Phys., Vol. 97, pp 249-310, 1991.

2 YEE, H.C., SWEBY, P.K. — Dynamical Approach Study of Spurious Steady-State Numerical Solutions for Nonlinear Differential Equations, Part II, The Dynamics of Numerics of Systems of 2 × 2 ODEs and its Connections to Finite Discretizations of PDEs. RNR Technical Report RNR-92-008, March 1992.

3 LAFON, A., YEE, H.C. — Dynamical Approach Study of Spurious Steady-State Numerical Solutions of Nonlinear Differential Equations, Part III, The Effects of Nonlinear Source Terms and Bound-

ary Conditions in Reaction-Convection Equations. <u>NASA Technical Memorandum 103877</u>, July. 1991.

4 LAFON, A., YEE, H.C. — Dynamical Approach Study of Spurious Steady- State Numerical Solutions of Nonlinear Differential Equations, Part IV, Stability vs. Numerical Treatment of Nonlinear Source Terms. <u>ONERA/CERT Technical Memorandum</u>, Feb. 1992.

5 COYLE, J.M., FLAHERTY, J.E. & LUDWIG, R. — On the Stability of Mesh Equidistribution Strategies for Time–Dependent Partial Differential Equations. <u>J. Comput. Phys.</u>, Vol. 62, pp26-39, 1986.

6 BUDD, C.J., STUART, A.M., KOOMULLIL, G.P. YEE, H.C. — Numerical Solution Behaviour of Model Convection–Diffusion BVP with Grid Adaptation. <u>In preparation</u>.

7 DOEDEL, E. — <u>AUTO: Software for Continuation and Bifurcation Problems in Ordinary Differential Equations</u>, CIT Press, Pasadena, 1986.